

Aldose Reductase–Deficient Mice Are Protected From Delayed Motor Nerve Conduction Velocity, Increased c-Jun NH₂-Terminal Kinase Activation, Depletion of Reduced Glutathione, Increased Superoxide Accumulation, and DNA Damage

Eric C.M. Ho,^{1,2} Karen S.L. Lam,^{2,3} Yuk Shan Chen,^{1,4} Johnny C.W. Yip,¹ Meena Arvindakshan,¹ Shin-Ichiro Yamagishi,⁵ Soroku Yagihashi,⁵ Peter J. Oates,⁶ Craig A. Ellery,⁶ Stephen S.M. Chung,^{1,3,7} and Sookja K. Chung^{1,3,4}

The exaggerated flux through polyol pathway during diabetes is thought to be a major cause of lesions in the peripheral nerves. Here, we used aldose reductase (AR)-deficient (AR^{-/-}) and AR inhibitor (ARI)-treated mice to further understand the *in vivo* role of polyol pathway in the pathogenesis of diabetic neuropathy. Under normal conditions, there were no obvious differences in the innervation patterns between wild-type AR (AR^{+/+}) and AR^{-/-} mice. Under short-term diabetic conditions, AR^{-/-} mice were protected from the reduction of motor and sensory nerve conduction velocities observed in diabetic AR^{+/+} mice. Sorbitol levels in the sciatic nerves of diabetic AR^{+/+} mice were increased significantly, whereas sorbitol levels in the diabetic AR^{-/-} mice were significantly lower than those in diabetic AR^{+/+} mice. In addition, signs of oxidative stress, such as increased activation of c-Jun NH₂-terminal kinase (JNK), depletion of reduced glutathione, increase of superoxide formation, and DNA damage, observed in the sciatic nerves of diabetic AR^{+/+} mice were not observed in the diabetic AR^{-/-} mice, indicating that the diabetic AR^{-/-} mice were protected from oxidative stress in the sciatic nerve. The diabetic AR^{-/-} mice also excreted less 8-hydroxy-2'-deoxyguanosine in urine than diabetic AR^{+/+} mice. The structural abnormalities observed in the sural

nerve of diabetic AR^{+/+} mice were less severe in the diabetic AR^{-/-} mice, although it was only mildly protected by AR deficiency under short-term diabetic conditions. Signs of oxidative stress and functional and structural abnormalities were also inhibited by the ARI fidarestat in diabetic AR^{+/+} nerves, similar to those in diabetic AR^{-/-} mice. Taken together, increased polyol pathway flux through AR is a major contributing factor in the early signs of diabetic neuropathy, possibly through depletion of glutathione, increased superoxide accumulation, increased JNK activation, and DNA damage. *Diabetes* 55:1946–1953, 2006

Neuropathy is one of the most common complications associated with diabetes (1). Although the exact mechanism for the pathogenesis of this disease is not completely understood, several contributing factors have been proposed. They include increased glucose flux through the polyol pathway, increased production of reactive oxygen species by the mitochondrial respiratory chain, nonenzymatic glycation, protein kinase C (PKC) activation, and increased flux through the hexosamine pathway (2). Among these models, the polyol pathway, which consists of aldose reductase (AR; which reduces glucose to sorbitol with the aid of NADPH) and sorbitol dehydrogenase (which converts sorbitol to fructose using the cofactor NAD⁺) received the most attention.

Evidence for the involvement of AR in diabetic neuropathy emerged from studies showing that AR was present in the peripheral nerves and that sorbitol was accumulated in the nerves under diabetic conditions (3). In addition, increased AR activity by introducing the human AR transgene led to more severe diabetic neuropathy (4,5) and a decreased level of reduced glutathione (5). The key evidence, however, is that several AR inhibitors (ARIs) were shown to prevent the development of diabetic neuropathy by reducing sorbitol accumulation (6), restoring blood flow (7), and improving motor nerve conduction velocity (MNCV) (6–8). However, the polyol pathway model still remains controversial because it has been shown that the amount of ARI that normalized the nerve sorbitol level was

From the ¹Institute of Molecular Biology, The University of Hong Kong, Hong Kong, Special Administrative Region (SAR), China; ²Department of Medicine, The University of Hong Kong, Hong Kong, SAR, China; ³Research Centre of Heart, Brain, Hormone and Healthy Aging, The University of Hong Kong, Hong Kong, SAR, China; ⁴Department of Anatomy, The University of Hong Kong, Hong Kong, SAR, China; ⁵Department of Pathology, Hirosaki University School of Medicine, Hirosaki, Japan; ⁶Department of Cardiovascular and Metabolic Diseases, Pfizer Global Research and Development, Groton, Connecticut; and the ⁷Department of Physiology, The University of Hong Kong, Hong Kong, SAR, China.

Address correspondence and reprint requests to Dr. S.K. Chung, Department of Anatomy, The University of Hong Kong, Hong Kong, SAR, China. E-mail: skchung@hkucc.hku.hk.

Received for publication 15 November 2005 and accepted in revised form 28 March 2006.

AR, aldose reductase; ARI, AR inhibitor; DHE, dihydroethidium; ERK, extracellular signal-regulated kinase-1; JNK, c-Jun NH₂ terminal kinase; MAPK, mitogen-activated protein kinase; MNCV, motor nerve conduction velocity; PAR, poly(ADP-ribose); PARP, PAR polymerase; PKC, protein kinase C; SNCV, sensory nerve conduction velocity; YFP, yellowish-green fluorescent protein.

DOI: 10.2337/db05-1497

© 2006 by the American Diabetes Association.

The costs of publication of this article were defrayed in part by the payment of page charges. This article must therefore be hereby marked "advertisement" in accordance with 18 U.S.C. Section 1734 solely to indicate this fact.

insufficient to normalize MNCV and nerve blood flow in diabetic rats (9).

The role of AR or the polyol pathway in diabetic neuropathy is not well understood. Previous studies demonstrated that hyperglycemia-induced oxidative stress led to the activation of mitogen-activated protein kinase (MAPK), which might contribute to the pathogenesis of this disease (10,11). Fidarestat, an ARI, was shown to prevent diabetes-induced activation of MAPK and nerve conduction velocity deficits (12), suggesting that ARIs would reduce the oxidative stress associated with diabetes. Moreover, using AR gene knockout mice (13), we have shown that AR deficiency could prevent diabetes-induced oxidative stress in nerve cells in retina (14). In addition, AR deficiency also prevented vascular abnormalities in the retina from the diabetic mice (14), suggesting that AR might contribute to diabetes-induced vascular dysfunction, which has been shown to contribute to the pathogenesis of diabetic neuropathy (15). Reduced sural endoneurial oxygen tension and diminished endoneurial blood flow have been demonstrated in diabetic animals and patients (16, 17). Increased polyol pathway activity is thought to be one of the major contributors to abnormal vascular tones in diabetic animals because it could activate PKC (18,19).

To further understand the role of AR in the pathogenesis of diabetic neuropathy, we examined the effect of AR deficiency on diabetic neuropathy by making use of AR^{-/-} mice (13) because AR mRNA and activity are present in the mouse sciatic nerve (5,20), and sorbitol can be further accumulated in the sciatic nerve under diabetic conditions (21). The effects of an ARI, fidarestat (SNK-860; Sanwa, Nagoya, Japan), on nerve conduction velocities, signs of oxidative stress, and nerve morphologic abnormalities were also investigated in diabetic AR^{+/+} mice and compared with those in diabetic AR^{-/-} mice. Here, we found that AR deficiency and AR inhibition reduced oxidative stress in the peripheral nerves and markedly protected mice from diabetes-induced functional deficits.

RESEARCH DESIGN AND METHODS

AR^{+/+} and AR^{-/-} mice generated previously (13) and backcrossed to C57BL/6N for more than five generations were used. Animal experiments were carried out under guideline set forth by the committee on the use of live animals in teaching and research at the University of Hong Kong.

Diabetes induction. Mice (6 weeks old, 20–25 g) were induced to become diabetic with streptozotocin (in 0.1 mol/l citrate buffer, pH 4.5; Sigma, St. Louis, MO) by injection (200 mg/kg body wt i.p.). Control animals were injected with citrate buffer. Blood glucose was monitored with a glucose meter (Bayer, Leverkusen, Germany) 2 days later. Mice with a blood glucose level >25 mmol/l were considered diabetic, and those with blood glucose level <8 mmol/l were considered nondiabetic.

Nerve conduction velocity measurement. The 4, 8, and 12 weeks' diabetic AR^{-/-} mice and their appropriate control animals were anesthetized with Hypnorm (Janssen, Oxford, U.K.)/Hypnorval (Hoffmann-La Roche, Nutley, NJ) at a concentration of 0.1 ml per 10 g body wt (the resulting mixture of Hypnorm/Dormicum contained 1.25 mg/ml midazolam, 2.5 mg/ml flunitrazepam, and 0.079 mg/ml fentanyl). Body temperature was maintained automatically at a mean rectal temperature of 37.5–37.9°C by the use of a heat pad (Fine Science Tools, Vancouver, BC, Canada). The sciatic nerve was stimulated (5–10 V, 0.05 ms single square-wave pulses) proximally at the level of the sciatic notch and distally at the level of the ankle with platinum needle electrodes (Grass, Quincy, MA). Compound muscle action potentials were recorded from the ipsilateral foot between digits 1 and 2, amplified, stored, and displayed on a computer (Spike 2; CED, Cambridge, U.K.). The first compound action potential from individual stimulation was used for the measurement of motor latency, whereas the second one was used for the measurement of sensory latency. Averaged distal and proximal motor and sensory latencies from 10 separate recordings, together with the nerve length between the two stimulation sites, were used for calculation of MNCV and sensory nerve conduction velocity (SNCV).

Carbohydrate measurement by high-performance liquid chromatography. The sciatic nerves of 4 weeks' diabetic AR^{-/-} mice and their appropriate control animals were dissected and frozen in liquid nitrogen until processed. Dry weight of the sciatic nerves was determined after drying the nerves in a SpeedVac (AS160; Savant Instruments, Farmingdale, NY) until the weight was constant. Carbohydrates were extracted from sciatic nerves of mice as described previously (22). Carbohydrate extracts were separated on a DX500 high-performance liquid chromatography system (Dionex, Sunnyvale, CA) equipped with a CarboPac (MA-1) anion exchange column (Dionex) with isocratic elution by 420 mmol/l NaOH. Peak integration was performed, using Peaknet software (Dionex). The peak areas were normalized with the internal control, and carbohydrates were quantified against a known standard curve run in the same run. The concentrations of carbohydrates were expressed in nanomoles per milligram dry weight of sciatic nerves.

Determination of glutathione level. Sciatic nerves were stored in liquid nitrogen until homogenization in 1 ml ice-cold 6% perchloric acid. After centrifugation at 4,000g for 10 min, nerve perchloric extracts were neutralized by 5 mol/l potassium carbonate and centrifuged at 4,000g for 5 min. The supernatant was then mixed with 0.89 ml of 20 mmol/l EDTA in 1 mol/l Tris-Cl buffer (pH 8.1). The reaction was initiated by the addition of 0.01 ml of *O*-pathaldehyde (10 mg in 1 ml methanol; Sigma). Reaction products were detected/quantified by fluorescence spectroscopy at λ -excitation 345 nm and λ -emission 425 nm (23).

Detection of superoxide. Dihydroethidium (DHE; 2 μ mol/l; Molecular Probes, Eugene, OR) was typically applied onto 6- μ m cryosections of tissue-freezing medium embedded sciatic nerves, incubated in a humidified chamber at 37°C (30 min, in dark). Sections were counterstained with 4',6'-diamidino-2-phenylindole dihydrochloride hydrate (DAPI; Sigma). Signals were captured with an Olympus IX71 microscope equipped with a Spot RT digital camera (Diagnostic Instruments, Detroit, MI).

Poly(ADP-ribose) immunostaining. The 10- μ m longitudinal paraffin-embedded sections of 4% paraformaldehyde-fixed sciatic nerves from 12 weeks' diabetic AR^{-/-} mice and their appropriate control mice were deparaffinized in xylene and pretreated with 0.3% H₂O₂ to eliminate endogenous peroxidase activity. Mouse monoclonal anti-poly(ADP-ribose) (PAR) antibody (Alexis, San Diego, CA) was applied onto the sections at a concentration of 1:200 overnight at 4°C. PAR immunoreactivity was detected with a biotinylated anti-mouse secondary antibody and streptavidin-biotin-peroxidase complex according to the instructions from Vector Elite kit (Vector Laboratories, Burlingame, CA). Diaminobenzidine was used as substrate for peroxidase. Sections were then counterstained with hematoxylin, dehydrated, and mounted. Images were captured with an Olympus IX71 microscope equipped with a Spot RT digital camera (Diagnostic Instruments).

Protein analyses using Western blotting. Sciatic nerves stored in liquid nitrogen were homogenized in ice-cold 0.1 mol/l NaCl, 0.05 mol/l Tris-Cl (pH 7.4), 0.001 mol/l EDTA, and a mixture of protease inhibitors (5 μ l/ml Complete; Roche, Basel, Switzerland). SDS-PAGE (8, 10, and 15% acrylamide) was performed with 50 μ g of total proteins. Separated proteins were transferred to a reinforced nitrocellulose membrane (Schleicher & Schuell, Dassel, Germany) using a "tank" buffer system (Bio-Rad, Hercules, CA). Primary antibodies used were antibodies against total p46 c-Jun NH₂-terminal kinase (JNK; 1:1,000; Santa Cruz Biotechnology, Santa Cruz, CA), antibodies against phosphorylated p54 JNK and phosphorylated p46 JNK (1:1,000, phosphorylated on Thr-183 and Tyr-185; Cell Signaling Technology, Danvers, MA), antibodies against total extracellular signal-regulated kinase-1 (ERK1) and ERK2 (1:1,000; Cell Signaling Technology), and antibodies against phosphorylated ERK1 and ERK2 (1:1,000, phosphorylated on Tyr-204; Santa Cruz Biotechnology). Detection was achieved using enhanced chemiluminescence Western blotting detection reagents (Amersham Biosciences, Buckinghamshire, U.K.). The immunoblots were scanned on a flatbed scanner (UMAX, Dallas, TX) and converted into numerical values by ImageQuant (version 5.1; Amersham Biosciences, Sunnyvale, CA).

Detection of yellowish-green fluorescent protein fluorescent nerve fibers. AR^{+/+} and AR^{-/-} mice (13) were mated with *thy1-YFP* mice (24,25) to introduce yellowish-green fluorescent protein (YFP) into sensory/motor neurons and their processes for analyzing the effect of AR deficiency on the organization of peripheral nerves in live animals. The images of fluorescent YFP nerve fibers in the ear, abdomen, diaphragm, and lower leg of these mice under normal conditions were captured with a digital camera (DC500; Leica, Bensheim, Germany) that was attached to a fluorescence stereomicroscope (MZ FLIII; Leica).

Morphometric analysis of sural nerves. Sural nerves were fixed in 2.5% glutaraldehyde and postfixed in 1% osmium tetroxide. After dehydration, midportions of the fixed sural nerves were embedded in epon and polymerized, and 1- μ m-thick transverse nerve sections were stained with toluidine blue. Fascicular area and myelinated fiber number and size were measured at a magnification of 1,600 \times using a computer-assisted image analyzing system

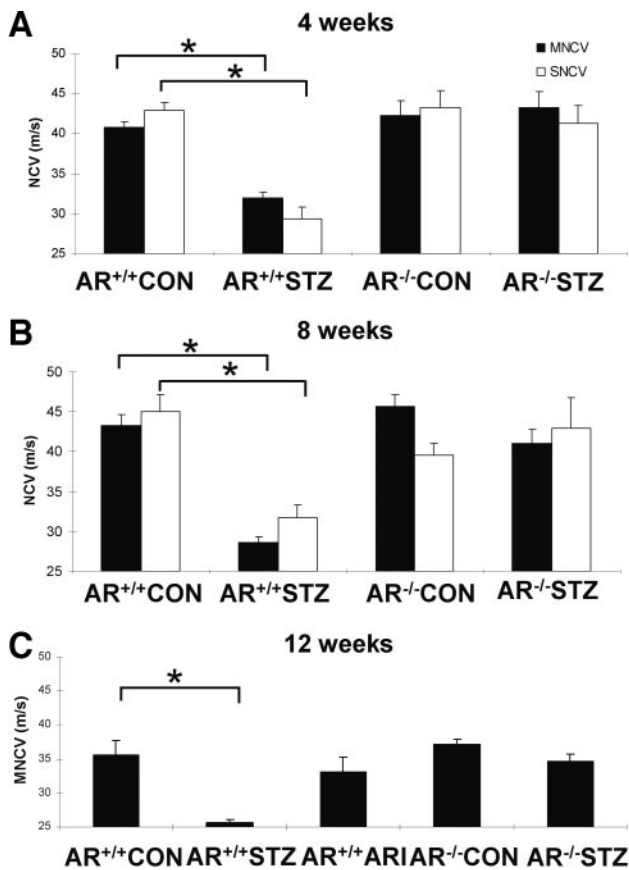


FIG. 1. Bar graphs showing that MNCV and SNCV deficits were protected by AR deficiency or AR inhibition. At 4 (A), 8 (B), and 12 (C) weeks of diabetes, MNCV/SNCV was reduced significantly in the diabetic AR^{+/+} mice. Reduction of MNCV and SNCV were not observed in diabetic AR^{-/-} mice or in ARI-treated diabetic AR^{+/+} mice. **P* < 0.001 by one-way ANOVA. For 4 and 8 weeks, *n* = 10–12 per group; for 12 weeks, *n* = 5–8 per group. AR^{+/+}ARI, ARI-treated diabetic AR^{+/+} mice; CON, control mice; NCV, nerve conduction velocity; STZ, streptozotocin-induced diabetic mice.

(National Institutes of Health image, Agfa Arcusscanner connected to a Quadra 700; Macintosh, Cupertino, CA).

Statistical analysis. All data are the means ± SE. Either Student's *t* test or one-way ANOVA together with Bonferroni's post hoc test were performed. *P* < 0.05 was considered statistically significant.

RESULTS

The AR^{-/-} mice backcrossed to C57BL/6N for at least five generations had mild impairment in water reabsorption in the kidney, leading to slightly increased urine output and increased water consumption, as described previously (13). Under diabetic conditions, there was no significant difference in the urine output, water consumption, and

level of blood glucose between AR^{-/-} and AR^{+/+} mice (data not shown).

AR deficiency prevented diabetes-induced MNCV and SNCV reduction. There was no significant difference in MNCV and SNCV between nondiabetic AR^{+/+} and AR^{-/-} mice. However, after 4, 8, and 12 weeks of diabetes, AR^{+/+} mice showed a significant reduction of MNCV compared with their nondiabetic counterparts (*P* < 0.001 for each stage). However, a significant reduction of MNCV in diabetic AR^{-/-} mice was not observed (Fig. 1). Similarly, the reduction of SNCV observed in diabetic AR^{+/+} mice (*P* < 0.001 for each stage) was also not observed in diabetic AR^{-/-} mice (Fig. 1). Not surprisingly, the ARI fidarestat also protected diabetic AR^{+/+} mice from a reduction of MNCV almost equivalent to that of AR-deficient mutants after 12 weeks of diabetes (Fig. 1).

Effects of AR deficiency on glucose and its related metabolites in the sciatic nerve. Nerve glucose levels in nondiabetic AR^{+/+} and AR^{-/-} mice were indistinguishable (Table 1). After 4 weeks of diabetes, both diabetic AR^{+/+} and AR^{-/-} mice showed significant increases in glucose content compared with their nondiabetic counterparts (*P* < 0.001). Glucose content in diabetic AR^{+/+} mice was not significantly different from that of diabetic AR^{-/-} mice (Table 1).

Under normal conditions, sorbitol and fructose contents in the sciatic nerves of AR^{-/-} mice were significantly reduced when compared with that of AR^{+/+} mice (*P* < 0.001). After 4 weeks of diabetes, both AR^{+/+} and AR^{-/-} mice showed significant increases in sorbitol and fructose in their sciatic nerves compared with those of the nondiabetic control animals (*P* < 0.001). Sorbitol and fructose levels in diabetic AR^{-/-} mice were significantly lower than that in diabetic AR^{+/+} mice (*P* < 0.001). The *myo*-inositol levels between nondiabetic AR^{+/+} and AR^{-/-} mice were similar. The *myo*-inositol levels in diabetic AR^{+/+} and AR^{-/-} mice were not statistically different from their nondiabetic counterparts (Table 1).

Diabetes-induced glutathione depletion in sciatic nerves was attenuated by AR deficiency. Glutathione levels in nondiabetic AR^{+/+} and AR^{-/-} mice were similar. A significant reduction of glutathione in the 4 weeks' diabetic AR^{+/+} mice was observed (*P* < 0.001), but no reduction in glutathione level was found in diabetic AR^{-/-} mice. The sciatic nerves of 12 weeks' diabetic AR^{-/-} mice or ARI-treated diabetic mice also showed similar protection from the depletion of reduced glutathione in the sciatic nerves (Fig. 2). Also, we found a significant increase in the urine 8-OHdG (8-hydroxy-2'-deoxyguanosine) content in 8 weeks' diabetic AR^{+/+} mice, but the increase was not statistically significant in diabetic AR^{-/-} mice (data not shown).

TABLE 1

Sugar and polyol levels in sciatic nerves of AR^{-/-} and AR^{+/+} mice after 4 weeks of diabetes

	<i>n</i>	Carbohydrate concentration (nmol/mg dry wt)			
		Glucose	Sorbitol	Fructose	<i>myo</i> -inositol
AR ^{+/+} nondiabetic	6	7.75 ± 1.90	1.02 ± 0.08	0.33 ± 0.04	17.88 ± 1.76
AR ^{+/+} STZ	6	57.32 ± 2.54*	1.68 ± 0.13*	1.85 ± 0.24*	19.63 ± 0.83
AR ^{-/-} nondiabetic	6	11.05 ± 1.96	0.34 ± 0.11*	0.12 ± 0.04*	16.06 ± 0.96
AR ^{-/-} STZ	6	60.04 ± 7.69†	0.81 ± 0.07†‡	0.53 ± 0.09†‡	20.21 ± 1.73

Data are means ± SE. **P* < 0.001 when compared with AR^{+/+} nondiabetic mice; †*P* < 0.001 when compared with AR^{-/-} nondiabetic mice; ‡*P* < 0.001 when compared with AR^{-/-} streptozotocin-induced diabetic mice (STZ). Statistics were performed by one-way ANOVA.

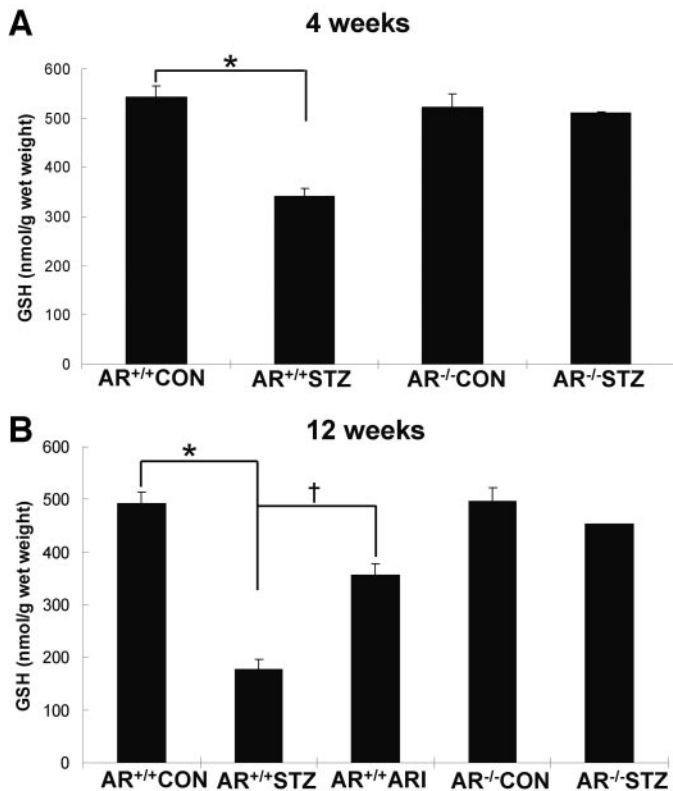


FIG. 2. Bar graphs showing that glutathione (GSH) reduction was prevented in diabetic $AR^{-/-}$ mice. At 4 (A) and 12 (B) weeks of diabetes, glutathione level was reduced in diabetic $AR^{+/+}$ mice, and a reduction of glutathione level was not observed in diabetic $AR^{-/-}$ mice. Similarly, reduction of glutathione level was partially ameliorated in ARI-treated diabetic $AR^{+/+}$ mice. * $P < 0.001$, † $P < 0.05$ by one-way ANOVA, $n = 5$ per group. $AR^{+/+}$ ARI, ARI-treated diabetic $AR^{+/+}$ mice; CON, control mice; STZ, streptozotocin-induced diabetic mice.

Diabetes-induced accumulation of superoxide was lower in the diabetic $AR^{-/-}$ mice. The oxidative fluorescent dye DHE, represented as red fluorescence in the nucleus of the cells, was used to determine the level of O_2^- in the sciatic nerve. Under normal conditions, ethidium fluorescence was barely detectable in the nuclei of cells from $AR^{+/+}$ and $AR^{-/-}$ mice (~6% of nuclei were positive for DHE). Sciatic nerves of 12 weeks' diabetic $AR^{+/+}$ mice showed a marked increase in DHE staining compared with that of nondiabetic $AR^{+/+}$ mice. The percentage of DHE-stained nuclei was also significantly increased ($P < 0.001$). However, the 12 weeks' diabetic $AR^{+/+}$ mice treated with ARI or fidarestat or the diabetic $AR^{-/-}$ animals showed much less accumulation of superoxide in the sciatic nerve (Fig. 3A). Quantitation results showed that the increase of DHE-positive nuclei as observed in diabetic $AR^{+/+}$ mice was ameliorated in ARI-treated diabetic $AR^{+/+}$ mice or diabetic $AR^{-/-}$ mice ($P < 0.001$) (Fig. 3B).

Diabetes-induced PAR polymerase activation was less in sciatic nerves of $AR^{-/-}$ mice. To further determine other indicators of oxidative stress, PAR polymerase (PARP) reactivity, which is induced by increased free radicals and DNA damage (2), was determined by PAR immunoreactivity in nucleus. PAR-reactive nuclei were barely detectable in the sciatic nerves of nondiabetic $AR^{+/+}$ and $AR^{-/-}$ mice. A marked increase in PAR immunoreactivity was observed in $AR^{+/+}$ mice after 12 weeks of diabetes. Moreover, 12 weeks' diabetic $AR^{-/-}$ mice were protected from PARP activation. In addition, oral treat-

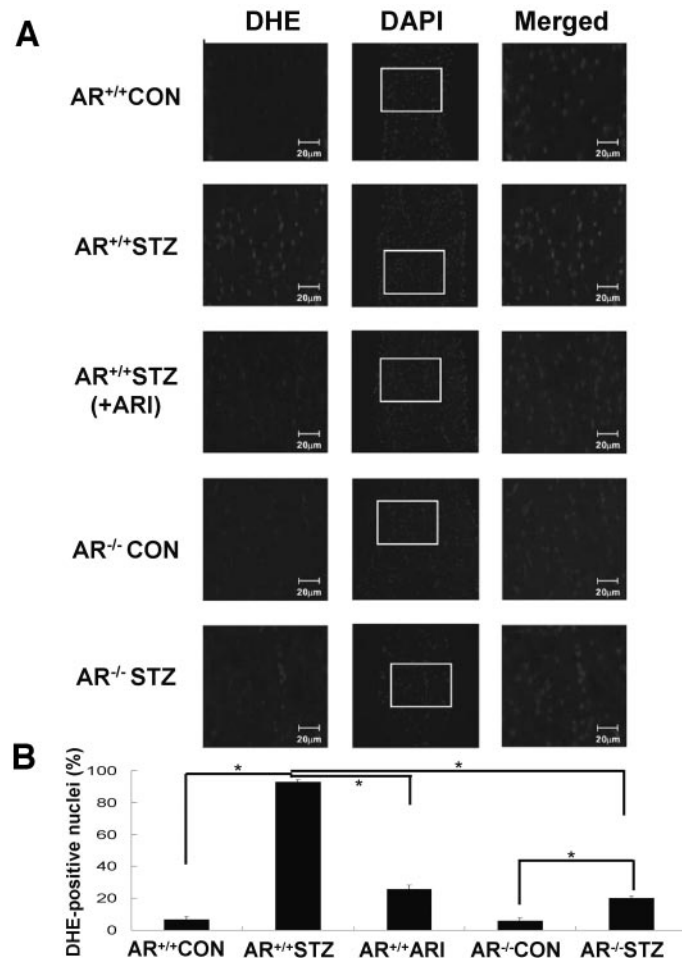


FIG. 3. A: Photomicrographs showing increase of DHE-stained superoxides in diabetic sciatic nerves was prevented in diabetic $AR^{-/-}$ mice or ARI-treated diabetic $AR^{+/+}$ mice. DHE-stained signals are in red, 4',6-diamidino-2-phenylindole dihydrochloride hydrate (DAPI)-stained nuclei are in blue, and merged signals are in purple. B: Bar graph showing increase of DHE-positive nuclei in sciatic nerves under diabetic conditions was prevented by AR deficiency or AR inhibition. * $P < 0.001$ by Student's t test, $n = 5$ per group. $AR^{+/+}$ ARI, ARI-treated diabetic $AR^{+/+}$ mice; CON, control mice; STZ, streptozotocin-induced diabetic mice.

ment with the ARI fidarestat during 12 weeks of diabetes protected $AR^{+/+}$ mice from PARP activation, similar to that observed in 12 weeks' diabetic $AR^{-/-}$ mice (Fig. 4). **Diabetes-induced activation of p46 JNK in the sciatic nerves was prevented by AR deficiency.** The expression level of p46 JNK in the sciatic nerve was similar in the nondiabetic $AR^{+/+}$ and $AR^{-/-}$ mice, and it was not affected by 4 weeks of diabetes in both groups of mice. The expression levels of phosphorylated p54 JNK and phosphorylated p46 JNK were also similar in the nondiabetic $AR^{+/+}$ and $AR^{-/-}$ mice. After 4 weeks of diabetes, there was a significant increase in the ratio of phosphorylated protein to total protein of p46 JNK in the diabetic $AR^{+/+}$ mice when compared with the nondiabetic $AR^{+/+}$ mice ($P < 0.001$). However, the phosphorylated protein-to-total protein ratio of p46 JNK in the $AR^{-/-}$ mice was unchanged after 4 weeks of diabetes. Unlike p46 JNK, the phosphorylated protein-to-total protein ratio of p54 JNK was not affected after 4 weeks of diabetes in both $AR^{+/+}$ and $AR^{-/-}$ mice (Fig. 5). Similar analysis was also made for ERK activation, but there was no significant difference between experimental groups (data not shown).

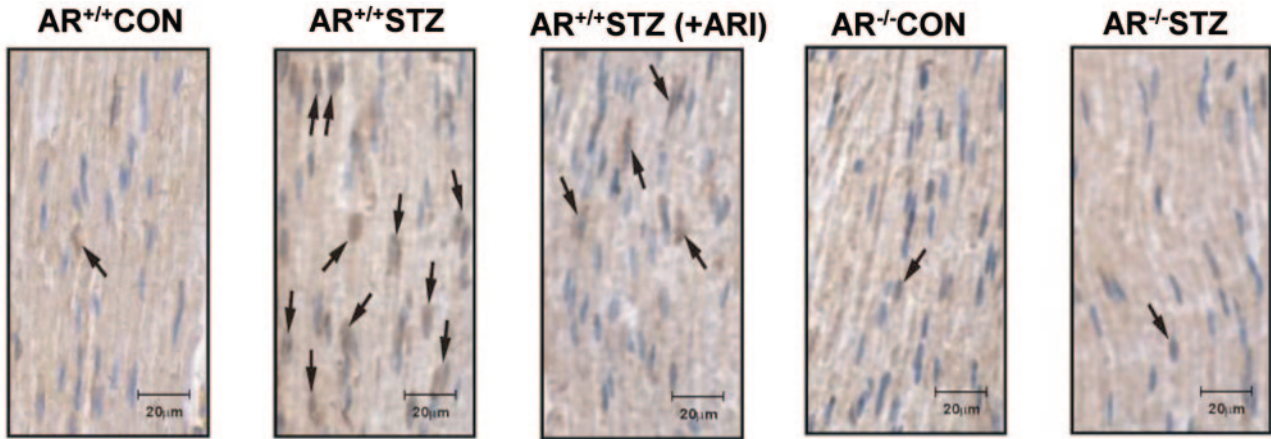


FIG. 4. Photomicrographs showing the increase in PAR-immunostained signals was ameliorated in diabetic $AR^{-/-}$ mice or ARI-treated diabetic $AR^{+/+}$ mice. Arrows point to PAR-positive nuclei. $n = 4-5$ per group. CON, control mice; STZ, streptozotocin-induced diabetic mice.

Diabetes-induced structural abnormalities in the sural nerves were partially prevented by AR deficiency. Under normal conditions, AR deficiency did not affect the structure of nerves, as indicated by the comparison of the total fascicular area, myelinated fiber size, and total myelinated fiber of the sural nerves of $AR^{+/+}$ and $AR^{-/-}$ mice (Table 2). These findings were also confirmed by analyzing the peripheral nerves of live $AR^{-/-}$ mice mated with *thy1-YFP* transgenic mice, which have YFP protein expression in all motor and sensory neurons, including the sural nerves, and allow direct viewing of nerves in the live animals. The gross innervation patterns of major organs at all the ages studied (4, 8, 12, and 24

weeks), such as abdomen, diaphragm, kidney, bladder, ear, and lower leg, in $AR^{-/-}$ mice were not obviously different from those of $AR^{+/+}$ mice under normal conditions (Fig. 6), suggesting that AR deficiency does not affect the normal development of the nervous system.

In the $AR^{+/+}$ mice, 8 weeks of diabetes caused a significant reduction in total fascicular area, mean myelinated fiber size, and fiber number (Table 2). Similar changes in these morphologic parameters were also observed after 12 weeks of diabetes. In the $AR^{-/-}$ mice, 8 or 12 weeks of diabetes did not cause a significant reduction in fascicular area and fiber number. Mean myelinated fiber size, however, was reduced after 8 or 12 weeks of diabetes. The effect of ARI on diabetes-induced structural changes of the nerves was also tested in wild-type mice. The results showed that mice with 12 weeks of diabetes treated with ARI also showed a reduction in fascicular area and mean myelinated fiber size (Table 2). However, the reduction in fascicular area was less severe than that found in diabetic mice not treated with ARI. Furthermore, ARI treatment also protected the nerve against diabetes-induced fiber loss. However, there was no significant difference in fascicular area or total fiber number in the sural nerves from 8 and 12 weeks' diabetic $AR^{-/-}$ and $AR^{+/+}$ mice or 12 weeks' diabetic $AR^{+/+}$ mice treated with ARI.

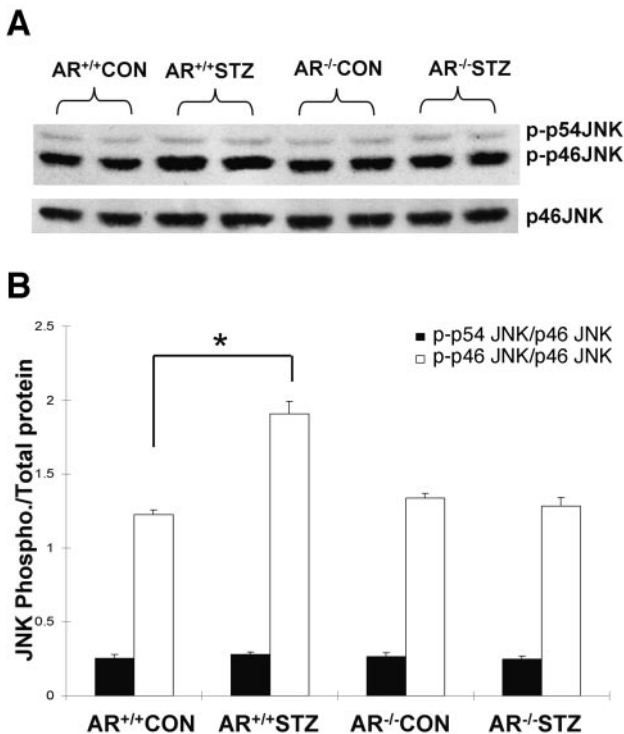


FIG. 5. A: Photomicrographs showing phosphorylated JNK and total JNK protein expression in $AR^{+/+}$ and $AR^{-/-}$ mice under control and diabetic conditions. B: Quantitation result showing that the phosphorylated p46 JNK-to-total p46 JNK protein ratio was increased in sciatic nerves of diabetic $AR^{+/+}$ mice but not in diabetic $AR^{-/-}$ mice. $n = 9$ per group. * $P < 0.001$ by one-way ANOVA. CON, control mice; STZ, streptozotocin-induced diabetic mice.

DISCUSSION

As previously described, AR-deficient mice had a mild impairment in water reabsorption in the kidney, leading to slightly increased urine output and increased water consumption under normal conditions without affecting the levels of serum electrolytes (13). However, under diabetic conditions, there was no significant difference in urine volume, water consumption, and blood and nerve glucose levels between $AR^{-/-}$ and $AR^{+/+}$ mice. In addition, morphometric analysis of sural nerve biopsies and gross comparisons of peripheral nerves of $AR^{+/+}$ or $AR^{-/-}$ mice mated with *thy1-YFP* transgenic mice showed no obvious effect of AR deficiency on the peripheral nervous system under normal conditions. Taken together, these observations indicate that the $AR^{-/-}$ mouse model would be an invaluable model for studying the role of AR deficiency in the pathogenesis of diabetic neuropathy.

Previous studies using ARIs in experimental animal models (4,8) and diabetic patients (26) showed that inhibition of AR activity could partially restore MNCV slowing,

TABLE 2
Morphologic data of myelinated nerve fibers in the sural nerves of AR^{-/-} and AR^{+/+} mice after 8 and 12 weeks of diabetes

	8 weeks				12 weeks			
	Total fascicular area (μm ²)	Mean myelinated fiber size (μm ²)	Total fiber number	n	Total fascicular area (μm ²)	Mean myelinated fiber size (μm ²)	Total fiber number	n
AR ^{+/+} nondiabetic	14,300 ± 672	13.22 ± 0.11	607.6 ± 28.1	9	14,640 ± 505	16.51 ± 0.29	535.6 ± 15.83	5
AR ^{+/+} STZ	12,410 ± 412*	12.41 ± 0.30*	543.8 ± 15.2*	6	11,700 ± 733†	14.86 ± 0.95*	491.7 ± 12.03*	5
AR ^{+/+} STZ ARI	ND	ND	ND	6	12,850 ± 839*	14.43 ± 0.43‡	512.0 ± 20.72	5
AR ^{-/-} nondiabetic	13,850 ± 292	13.82 ± 0.36	567.8 ± 20.8	9	15,270 ± 886	16.55 ± 0.72	537.3 ± 34.24	5
AR ^{-/-} STZ	13,070 ± 1,227	12.88 ± 0.22§	558.4 ± 40.5	7	14,150 ± 979	14.44 ± 0.56§	558.0 ± 25.63	5

Data are means ± SE. * $P < 0.05$, † $P < 0.01$, ‡ $P < 0.001$ when compared with AR^{+/+} nondiabetic mice; § $P < 0.05$ when compared with AR^{-/-} nondiabetic mice. Statistics were performed by Student's *t* test. ARI, fidarestat-treated mice; ND, not determined; STZ, streptozotocin-induced diabetic mice.

which is one of the major features of diabetic neuropathy. Transgenic mice that overexpress AR either ubiquitously (4) or specifically in Schwann cells (5) developed more severe MNCV deficits. Here, we demonstrated that diabetic AR^{-/-} mice were protected against MNCV and SNCV reduction. Furthermore, ARI (fidarestat) treatment protected diabetic AR^{+/+} mice from MNCV reduction, similar to its protective effect on SNCV reduction, as demonstrated by others (27). Our current data suggest that exaggerated flux through the polyol pathway plays a key role in the pathogenesis of acute diabetic neuropathy, possibly acting directly on the peripheral nerves. Although the AR level in mouse sciatic nerve is low (28), the presence of AR mRNA was clearly demonstrated (5). Furthermore, in diabetic mice, AR activity (5) and sorbitol accumulation (21) were found to be increased in this tissue. The low level of sorbitol in mouse sciatic nerve does not truly reflect the level of polyol pathway activity. We have previously shown that the sorbitol level in the sciatic nerves of diabetic C57BL/10N, nondiabetic, and diabetic sorbitol dehydrogenase-deficient mice were increased 4.3, 16.6, and 38.1-fold, respectively, above that of nondiabetic C57BL/10N mice (21), indicating that sorbitol is quickly converted to fructose by sorbitol dehydrogenase and that a significant amount of glucose is fluxed through the polyol pathway, particularly in the diabetic mice. Interestingly, trace amounts of sorbitol and fructose were found in the diabetic AR/sorbitol dehydrogenase double-mutant mice (data not shown) and the AR^{-/-} mice. These may be contributed by other proteins with AR-like activity, such as aldehyde reductase (29), the fibroblast growth factor-regulated protein gene (*Fgfrp*) (30), and the androgen-regulated vas deferens protein gene (*Avdp*) (30).

We found that the glutathione level was decreased in the sciatic nerves of diabetic AR^{+/+} mice, but not in diabetic AR^{-/-} or ARI-treated diabetic AR^{+/+} mice, indicating that AR activity contributes to hyperglycemia-induced glutathione depletion. Potential mechanisms of the polyol pathway's contribution to diabetes-induced oxidative stress have been discussed previously (2). The difference in the absolute level of glutathione reported here compared with that of the previous study (5) may be the result of differences in mouse substrains or the adaptation of a more sensitive detection method in the current study. Previous studies demonstrated that an increase of oxidative stress could lead to the activation of stress-activated protein kinases, such as MAPK (10). Our current data showed that diabetes caused a significant activation of p46 JNK in the sciatic nerves of wild-type mice, which was prevented by AR deficiency. It is likely that amelioration of oxidative stress by AR deficiency under diabetic conditions might contribute to attenuation of JNK activation in the sciatic nerve in AR^{-/-} mice because other signs of oxidative stress, such as superoxide accumulation (determined by DHE staining) or PARP activation (determined by PAR immunohistochemistry), in sciatic nerves observed in diabetic AR^{+/+} mice were also ameliorated in diabetic AR^{-/-} mice or ARI-treated diabetic AR^{+/+} mice. Taken together, our data suggest that AR is a key enzyme in the pathogenesis of diabetic neuropathy and that diabetes-induced oxidative stress might be primarily the consequence of increased flux of glucose through the polyol pathway in the nervous tissue, similar to nerve cells in the diabetic retina (14).

We observed small but significant loss of myelinated nerve fibers in our diabetic wild-type mice. Previous

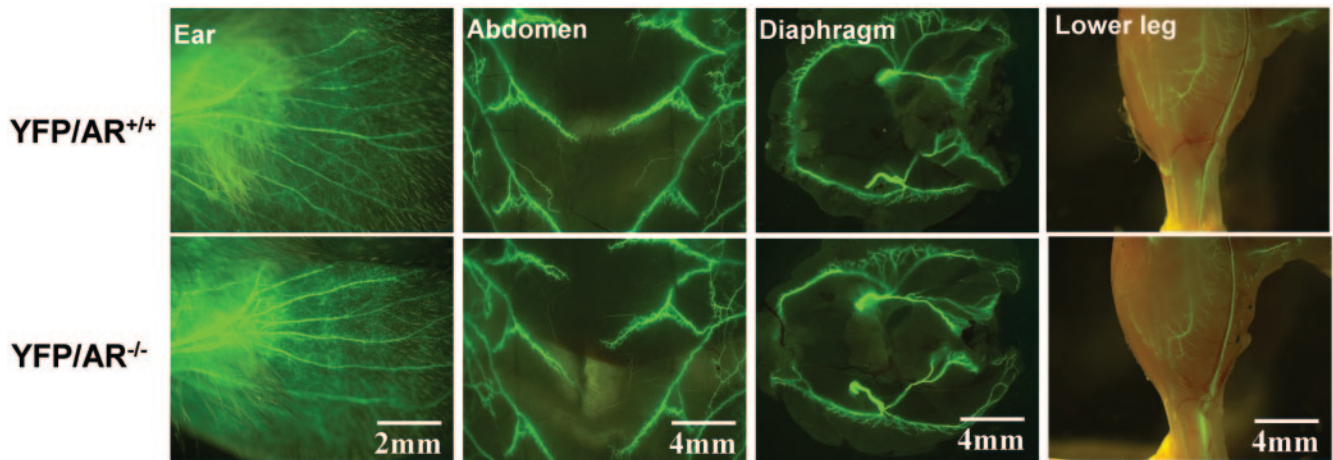


FIG. 6. Representative photographs showing no major difference in the innervation patterns of ear, abdomen muscle, diaphragm muscle, and lower leg between YFP/AR^{+/+} and YFP/AR^{-/-} mice under normal conditions. Mice presented here were 24 weeks old.

animal studies did not find such structural changes (4,31). This discrepancy may be due to the fact that the previous studies did not count all of the nerve fibers within the nerve fascicle. The diabetes-induced reduction of fascicular area and fiber number observed in the sural nerves of wild-type mice were largely attenuated in AR^{-/-} mice, indicating that AR activity contributes to these hyperglycemia-induced lesions. ARI treatment only partially alleviated these structural changes. This may be attributable to an insufficient amount of drug to completely inhibit AR in the target tissue. Interestingly, diabetes-induced reduction in mean myelinated fiber size was also not alleviated by an AR-deficiency mutation or ARI treatment, suggesting that other toxic effects of hyperglycemia, such as glycation or inappropriate activation of PKC, might contribute to this diabetes-induced structural change of the nerves. It is likely that diabetic neuropathy involves multiple pathogenic mechanisms.

Here, we demonstrate that AR or the polyol pathway plays a key role in the pathogenesis of diabetic neuropathy. Our AR^{-/-} mouse model is a useful model for determining its contribution to the cascade of molecular events, such as reduced number of cytoskeletons in distal axons (32–34), transport of cytoskeletons or nerve growth factors (34), or aberrant phosphorylation (35), to further explain the role of AR deficiency in functional, biochemical, and structural recovery of peripheral nerves. Of course, these AR-deficient mice can also serve to determine the interactions of AR with other hypothesized contributors to diabetic neuropathy, such as insulinopenia, impaired neurotrophic support, or glycation.

ACKNOWLEDGMENTS

This project was partly supported by grants from the Hong Kong Research Grant Council (HKU7313/04M) and the Biotechnology Research Institute, Hong Kong University of Science and Technology (to S.K.C.).

REFERENCES

1. Thomas PK: Diabetic peripheral neuropathies: their cost to patient and society and the value of knowledge of risk factors for development of interventions. *Eur Neurol* 41 (Suppl. 1):35–43, 1999
2. Brownlee M: Biochemistry and molecular cell biology of diabetic complications. *Nature* 414:813–820, 2001
3. Gabbay KH, Merola LO, Field RA: Sorbitol pathway: presence in nerve and cord with substrate accumulation in diabetes. *Science* 151:209–210, 1966
4. Yagihashi S, Yamagishi SI, Wada RiR, Baba M, Hohman TC, Yabe-Nishimura C, Kokai Y: Neuropathy in diabetic mice overexpressing human aldose reductase and effects of aldose reductase inhibitor. *Brain* 124: 2448–2458, 2001
5. Song Z, Fu DT, Chan YS, Leung S, Chung SS, Chung SK: Transgenic mice overexpressing aldose reductase in Schwann cells show more severe nerve conduction velocity deficit and oxidative stress under hyperglycemic stress. *Mol Cell Neurosci* 23:638–647, 2003
6. Tomlinson DR, Moriarty RJ, Mayer JH: Prevention and reversal of defective axonal transport and motor nerve conduction velocity in rats with experimental diabetes by treatment with the aldose reductase inhibitor Sorbinil. *Diabetes* 33:470–476, 1984
7. Nakamura J, Kato K, Hamada Y, Nakayama M, Chaya S, Nakashima E, Naruse K, Kasuya Y, Mizubayashi R, Miwa K, Yasuda Y, Kamiya H, Ienaga K, Sakakibara F, Koh N, Hotta N: A protein kinase C- β -selective inhibitor ameliorates neural dysfunction in streptozotocin-induced diabetic rats. *Diabetes* 48:2090–2095, 1999
8. Yue DK, Hanwell MA, Satchell PM, Turtle JR: The effect of aldose reductase inhibition on motor nerve conduction velocity in diabetic rats. *Diabetes* 31:789–794, 1982
9. Cameron NE, Cotter MA, Dines KC, Maxfield EK, Carey F, Mirrlees DJ: Aldose reductase inhibition, nerve perfusion, oxygenation and function in streptozotocin-diabetic rats: dose-response considerations and independence from a myo-inositol mechanism. *Diabetologia* 37:651–663, 1994
10. Wang X, Martindale JL, Liu Y, Holbrook NJ: The cellular response to oxidative stress: influences of mitogen-activated protein kinase signalling pathways on cell survival. *Biochem J* 333 (Pt. 2):291–300, 1998
11. Purves T, Middlemas A, Agthong S, Jude EB, Boulton AJ, Fernyhough P, Tomlinson DR: A role for mitogen-activated protein kinases in the etiology of diabetic neuropathy. *FASEB J* 15:2508–2514, 2001
12. Price SA, Agthong S, Middlemas AB, Tomlinson DR: Mitogen-activated protein kinase p38 mediates reduced nerve conduction velocity in experimental diabetic neuropathy: interactions with aldose reductase. *Diabetes* 53:1851–1856, 2004
13. Ho HT, Chung SK, Law JW, Ko BC, Tam SC, Brooks HL, Knepper MA, Chung SS: Aldose reductase-deficient mice develop nephrogenic diabetes insipidus. *Mol Cell Biol* 20:5840–5846, 2000
14. Cheung AK, Fung MK, Lam TT, So KT, Chung SS, Chung SK: Aldose reductase deficiency prevents diabetes-induced blood-retinal barrier breakdown, apoptosis, and glial reactivation in the retina of *db/db* mice. *Diabetes* 54:3119–3125, 2005
15. Gooch C, Podwall D: The diabetic neuropathies. *Neurologist* 10:311–322, 2004
16. Cameron NE, Eaton SE, Cotter MA, Tesfaye S: Vascular factors and metabolic interactions in the pathogenesis of diabetic neuropathy. *Diabetologia* 44:1973–1988, 2001
17. Newrick PG, Wilson AJ, Jakubowski J, Boulton AJ, Ward JD: Sural nerve oxygen tension in diabetes. *Br Med J (Clin Res Ed)* 293:1053–1054, 1986
18. Xia P, Kramer RM, King GL: Identification of the mechanism for the inhibition of Na⁺,K⁺-adenosine triphosphatase by hyperglycemia involving activation of protein kinase C and cytosolic phospholipase A2. *J Clin Invest* 96:733–740, 1995

19. Oates PJ: Polyol pathway and diabetic peripheral neuropathy. *Int Rev Neurobiol* 50:325-392, 2002
20. Fu DTW, Lee AYW, Lin CXF, Chung SSM, Chung SS: Downregulation of mouse aldose reductase mRNA in the Schwann cells but not in the endothelial cells of sciatic nerve by hyperglycemia. *Soc Neurosci Abs* 22:1498, 1996
21. Ng TF, Lee FK, Song ZT, Calcutt NA, Lee AY, Chung SS, Chung SK, Ng DT, Lee LW: Effects of sorbitol dehydrogenase deficiency on nerve conduction in experimental diabetic mice. *Diabetes* 47:961-966, 1998
22. Lal S, Szwergold BS, Taylor AH, Randall WC, Kappler F, Brown TR: Production of fructose and fructose-3-phosphate in maturing rat lenses. *Invest Ophthalmol Vis Sci* 36:969-973, 1995
23. Obrosova IG, Fathallah L, Lang HJ, Greene DA: Evaluation of a sorbitol dehydrogenase inhibitor on diabetic peripheral nerve metabolism: a prevention study. *Diabetologia* 42:1187-1194, 1999
24. Chen YS, Chung SSM, Chung SK: Noninvasive monitoring of diabetes-induced cutaneous nerve fiber loss and hypoalgesia in *thy1*-YFP transgenic mice. *Diabetes* 54:3112-3118, 2005
25. Feng G, Mellor RH, Bernstein M, Keller-Peck C, Nguyen QT, Wallace M, Nerbonne JM, Lichtman JW, Sanes JR: Imaging neuronal subsets in transgenic mice expressing multiple spectral variants of GFP. *Neuron* 28:41-51, 2000
26. Judzewitsch RG, Jaspán JB, Polonsky KS, Weinberg CR, Halter JB, Halar E, Pfeifer MA, Vukadinovic C, Bernstein L, Schneider M, Liang KY, Gabbay KH, Rubenstein AH, Porte D: Aldose reductase inhibition improves nerve conduction velocity in diabetic patients. *N Engl J Med* 308:119-125, 1983
27. Mizuno K, Kato N, Makino M, Suzuki T, Shindo M: Continuous inhibition of excessive polyol pathway flux in peripheral nerves by aldose reductase inhibitor fidarestat leads to improvement of diabetic neuropathy. *J Diabetes Complications* 13:141-150, 1999
28. Gui T, Tanimoto T, Kokai Y, Nishimura C: Presence of a closely related subgroup in the aldo-ketoreductase family of the mouse. *Eur J Biochem* 227:448-453, 1995
29. Sato S: Rat kidney aldose reductase and aldehyde reductase and polyol production in rat kidney. *Am J Physiol* 263:F799-F805, 1992
30. Ho HT, Jenkins NA, Copeland NG, Gilbert DJ, Winkles JA, Louie HW, Lee FK, Chung SS, Chung SK: Comparisons of genomic structures and chromosomal locations of the mouse aldose reductase and aldose reductase-like genes. *Eur J Biochem* 259:726-730, 1999
31. Zochodne DW, Sun H, Cheng C, Eyer J: Accelerated diabetic neuropathy in axons without neurofilaments. *Brain* 127:2193-2200, 2004
32. Pettersen JA, Zochodne DW, Bell RB, Martin L, Hill MD: Refractory neurosarcoidosis responding to infliximab. *Neurology* 59:1660-1661, 2002
33. Yagihashi S, Kamijo M, Watanabe K: Reduced myelinated fiber size correlates with loss of axonal neurofilaments in peripheral nerve of chronically streptozotocin diabetic rats. *Am J Pathol* 136:1365-1373, 1990
34. Sayers NM, Beswick LJ, Middlemas A, Calcutt NA, Mizisin AP, Tomlinson DR, Fernyhough P: Neurotrophin-3 prevents the proximal accumulation of neurofilament proteins in sensory neurons of streptozocin-induced diabetic rats. *Diabetes* 52:2372-2380, 2003
35. Fernyhough P, Gallagher A, Averill SA, Priestley JV, Hounsom L, Patel J, Tomlinson DR: Aberrant neurofilament phosphorylation in sensory neurons of rats with diabetic neuropathy. *Diabetes* 48:881-889, 1999